Evaluation of Ground Currents in a PV System with High Frequency Modeling

M.C. Di Piazza*, F. Viola**‡, G. Vitale*

* Consiglio Nazionale delle Ricerche, CNR – ISSIA UOS Palermo

Via U. La Malfa, 53 90146 Palermo Phone +39 0916809656

** Department of Energy, Information engineering, Mathematical models University of Palermo, Palermo, Italy

(dipiazza@pa.issia.cnr.it, fabio.viola@unipa.it, gianpaolo.vitale@cnr.it)

‡
Corresponding Author Fabio Viola; phone: +3909132860253, Viale delle Scienze, edificio 9, Parco d'Orleans, Palermo, Italy

Received: 24.04.2018 Accepted:22.06.2018

Abstract- In this work a high frequency model of a photovoltaic (PV) plant is identified and implemented aiming to investigate the common mode (CM) currents circulating through the ground connections of the plant. From the identification of the impedance obtained by frequency response of photovoltaic module and by a suitable of the power conversion unit, an equivalent high frequency circuit representation has been developed. The lumped parameters circuit model is implemented in PSpice environment to obtain the CM leakage currents. Harmonics at frequencies multiple of the switching frequency and a strong resonance at about 12 MHz are detected.

Keywords High frequency modelling, Parameter identification, Photovoltaic plants, Common mode currents.

1. Introduction

Usually, the power conversion unit (PCU) acts a fundamental role in photovoltaic plants, since it obtains the tracking of the maximum power coming from the collection of the solar panels and adapts the available energy in an appropriate form to feed the grid or to be employed by the customer or in islanded systems.

Numerous efforts have been devoted to realize a Maximum Power Point Tracking (MPPT) algorithms [1,2], and new power electronic sensors, devices and topologies [3-10].

The new technologies used in the high speed commutation inverters allow to increase the switching frequency of the power converters, reducing the size of inductors and capacitors and improving their power density [11], but they give rise to steep variations of voltage and current that bring different complications worsening the electromagnetic interference both radiated and conducted.

The overvoltages taking place at the inverter terminals, once long wire arrangements are employed, is one of the potential negative effects and it could become critical. In addition, one of the most serious disturbances is the common mode (CM) current, known also as "leakage current" or "ground current". This leakage currents flows through a path defined by the inverter, the DC cables the PV panels and the ground since both the PV panels and the inverter are connected to the ground by capacitive parasitic connections.

This current is responsible for electromagnetic interference (EMI) with other susceptible devices via the ground connection or for radiation phenomena since it contains high frequency components.

When the solar panels, the inverter and the grid connection, are distant from each other's, the parasitic capacitive coupling to the ground defines a multiple path in which the high frequency CM current can flow.

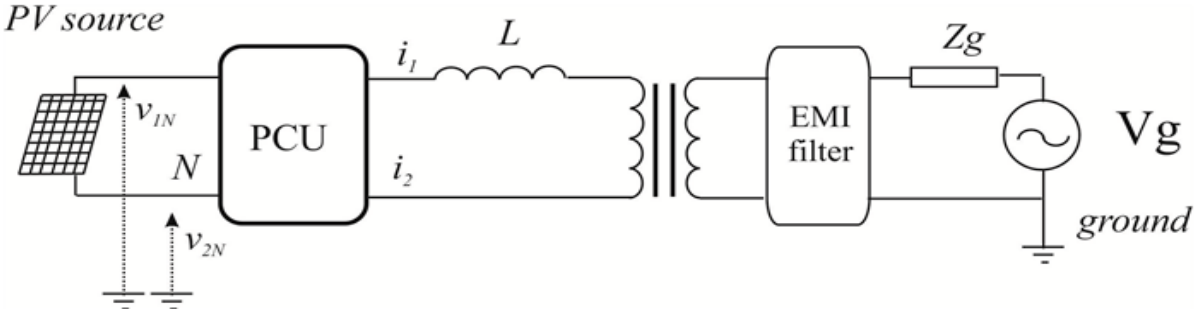

Fig. 1. General block diagram of a PV plant.

In technical literature limited number of works have addressed such aspects, nevertheless the CM current generation has been described. Araneo in [12] described phenomenon and coupling mechanisms in high power grid, defining an equivalent circuit and also through measurements. By defining domestic PV plants, in which no low frequency transform has been inserted, [13] and [14] highlighted that the presence of a galvanic connection between the grid and the plant allows the presence of higher CM currents, limited only by the EMI inverter filter. Both these papers propose a CM equivalent scheme for the single-phase grid connected inverter at medium frequency range and analyse several topologies.

This paper starts by focusing the attention on the role of parasitic components, stray capacitances in the PV panels and in the inverter, parasitic inductances in the wires connecting the inverter power devices and parasitic components inside power devices. Then an accurate high frequency modelling of the plant is defined, which allows the CM current to be predicted.

The paper is organized as follows: Section 2 describes the high frequency parasitic couplings taking place in a PV system; Section 3 is devoted to the experimental set-up used to recognize the PV module parasitic factors; Section 4 covers the informations about the PSpice application of the model for simulation; finally results are given and discussed in Section 5.

2. Photovoltaic Plant Layout

A PV plant involves PV source made by the series/parallel connections of PV modules and a PCU in which typically a DC/DC converter realizes the MPPT and the balance of voltage between the source output and the inverter input. An inverter follows the PCU, the resulting alternative waveform reaches the grid via a series inductance and a low frequency (LF) transformer. An EMI filter can be used to suppress the undesirable harmonics. The block diagram is sketched in Fig.1, where v_{1N} and v_{2N} are the phase-to-ground voltages, i_1 and i_2 are the currents on active conductors, L is the coupling line inductor, and vg with series impedance Zg represents the grid.

The current to be injected into the grid is given by the coupling inductance as the difference between the inverter voltage, seen as a voltage controlled source, and the grid voltage, divided by its impedance.

The transformer assures the galvanic insulation between the grid and the PV plant and prevents a DC current to be injected into the grid anyway it is expensive especially for low power applications and according to the Standards of some countries, it can be discarded. Such PV plants are known as transformerless plants.

With reference to Fig. 1, assumed the ground as common reference voltage, it is possible to define the CM voltage at the terminals of the inverter as:

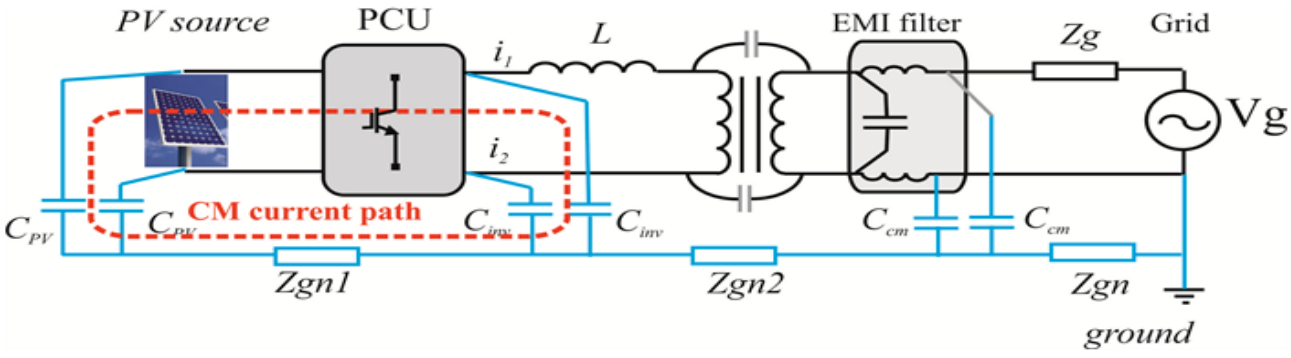

Fig. 2. High frequency representation of a PV plant.

$$v_{cm} = \frac{v_{1N} + v_{2N}}{2} \quad . \tag{1}$$

The differential mode (DM) voltage is the output inverter voltage:

$$v_{dm} = v_{1N} - v_{2N} = v_{12} \tag{2}$$

The CM current is the sum of the two line output current:

$$i_{cm} = i_1 + i_2 \tag{3}$$

and the DM current is given by:

$$i_{dm} = \frac{i_1 - i_2}{2} \tag{4}$$

The DM current corresponds to the current injected into the grid by the inverter, while the CM current flows through the parasitic capacitive couplings between the different parts of the PV plant and the ground connection. For this reason, it is known also as ground current.

The high frequency model of the PV plant, in which the CM return paths are highlighted, is shown in Fig. 2. These paths include stray capacitances between the PV panels and the ground Cpv, stray capacitances between the line output inverter and the ground Cinv and stray capacitances of the EMI filter, Ccm. The ground path impedance is indicated with Z_{gn}. It can be noted that the high frequency modelling points out all possible reclosing paths for CM current. The possible incidence of the low frequency transformer for the CM current is low, since transformer has a high impedance at CM current frequencies, so the main path to be investigated is formed by stray capacitances between the PV source and the inverter.

3. PV Module Parasitic Parameters Identification

In order to define the high frequency model schematized in Fig.2, the value of parasitic capacitance between the PV generator and the ground connection has to be determined. To this aim, an appropriate measurement-based parameter identification has to be performed, since the parasitic capacitance between the PV generator and the ground depends on real PV plant geometrical dimensions and installation characteristics.

In general, for developing a PV array high frequency model, the actual PV module connections have to be taken into account and measurements on the whole installation have to be performed to suitably consider the coupling with the metallic support and the ground.

In this study, the PV model parameter identification has been carried out for the case of a single silicon monocrystalline PV module whose plate data are presented in Table 1.

The used experimental setup is schematically illustrated in Fig. 3.

Table 1. Characteristics of the PV module

Nominal power [W]	P_n	20
Short circuit current [A]	I_{sc}	9.34
Open circuit voltage [V]	V_{oc}	21
Maximum power point current [A]	I_{MPP}	1.18
Maximum power point voltage [V]	V_{MPP}	16.8

It is composed of the following equipment:

- an Agilent 4285A precision LCR meter with the following features: frequency range 75kHz – 30 MHz, 0.1% basic accuracy, high-speed measurements (30 ms/meas.); it is connected between the two input terminals of the PV module and the ground connection;
- a PC where a dedicated software, implemented by LabView, controls the LCR meter for the acquisition of the measured impedance values from 75 kHz to 4 MHz; it uses a GPIB (IEEE 488) interface bus.

From the acquired measurements it is possible to observe that up to 500 kHz the impedance shows a purely capacitive behavior, whereas for higher frequencies an inductive contribution is present as well. The curve of the impedance magnitude vs. frequency is shown in Fig.4.

By means of a fitting procedure on measured data, in the range 100 kHz- 4 MHz, the parasitic capacitance value is calculated to be equal to 73 pF. Performing a further impedance measurement in the frequency range between 1 MHz and 7 MHz, only a parasitic inductance is individuated, whose value is about 1 µH. A small parasitic resistance due to the electrical connection is also detected but its contribution is neglected in this analysis.

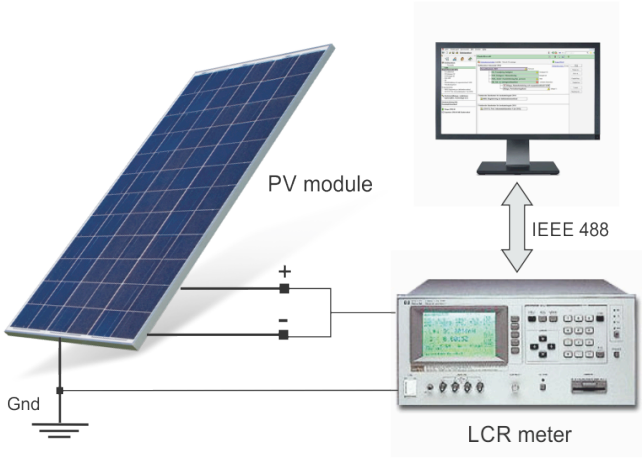

Fig. 3. Measurement setup used for the evaluation of a PV module parasitic components

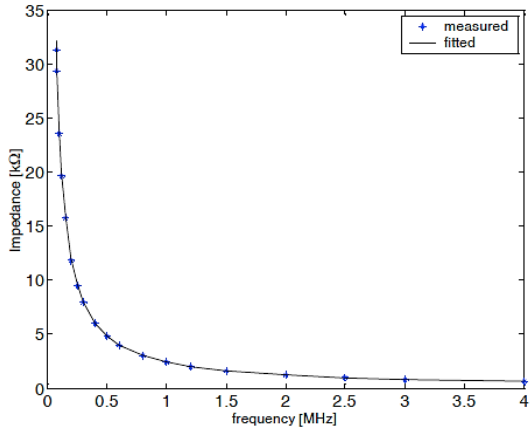

Fig.4. Measured impedance magnitude versus frequency

4. HF model Implementation

In this section, the PV plant shown in Figure 2 is described by its High Frequency model. The following parts have been analyzed: a) the PV array, b) the Power Conversion Unit, c) the power devices adopted into the PCU.

A. Model of the PV array

The voltage delivered by the arrangement of the PV panels has been chosen equal to about 500V in the maximum operating power point at a rated power of 1 kW. This voltage requires two parallel connected strings, each formed of 24 series connected modules. On the basis of this configuration the parasitic parameters previously determined for a single module have been re-calculated. The common mode current path will flow through all parasitic capacitors and inductors as parallel connected, hence, to obtain the HF parameters for the whole model arrangement, the parasitic capacitance of one module is multiplied and the parasitic inductance is divided for the number of utilized modules, respectively; these values are given in Table 2. The representation of the PV source to reproduce the power supplied to the PCU has been simplified since the analysis is focused on the evaluation of the ground currents propagation. It has been modelled by a real voltage generator model composed of the open circuit voltage generator and a series resistance RPV; it is calculated on the optimal operating point according to (5) and considering that the module gives at any instant at MPP Standard Test Conditions, a voltage equal to 16.8 V. In equation (5) Voc stands for open circuit voltage, Vmpp and Impp represent the maximum poer point voltage and current respectively. The PSpice model of the PV array is drawn in Fig. 5.

$$R_{PV}=\frac{V_{OC}-V_{mpp}}{I_{mpp}}=4\Omega \quad (5)$$

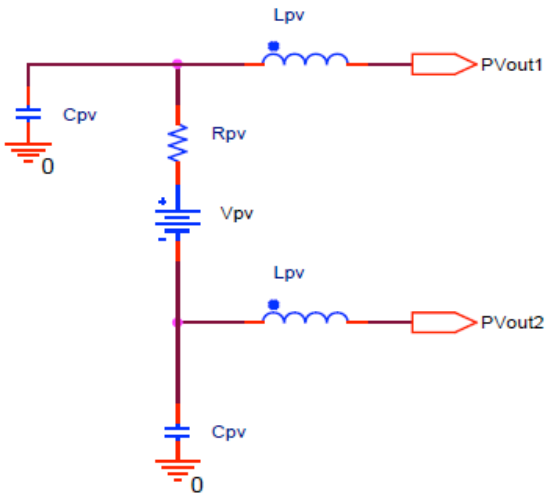

Fig.5. PSpice model of the PV array.

Table 2. Parasitic parameters of the PV array

Parasitic capacitance to ground [nF]	C_{pv}	1.75
Parasitic inductance of the connecting wires [nH]	L_{pv}	41.6

B. Model of the Power Conversion Unit

The power conversion unit employs Insulated Gate Bipolar Transistor (IGBT) as power switches. The IGBTs are characterized by high robustness and reliability and can be switched by a low power signal at the gate terminal for these reasons they are widely used in power conversion applications. A full-bridge single phase IGBT inverter with switching frequency of 10 kHz has been considered; it is formed by four IGBTs grouped in a unique power module. The high frequency circuit model of the inverter suitable to analyze the CM current propagation in the loop between the PV array and the inverter includes both the stray capacitance between the aluminum radiator of IGBT module and the ground (C_{inv}) and the stray inductance of the connecting wires of each leg of the inverter (L_{inv}). A precision RLC meter (Agilent 4285ALCR) with a frequency range between 150 kHz and 4 MHz has been used to measure the parasitic capacitances whereas inductance of the connecting wires Linv is evaluated using the analytical formula for two parallel cylindrical conductors. These parameters are summarized in table 3. Fig. 6 shows The PSpice model of the inverter.

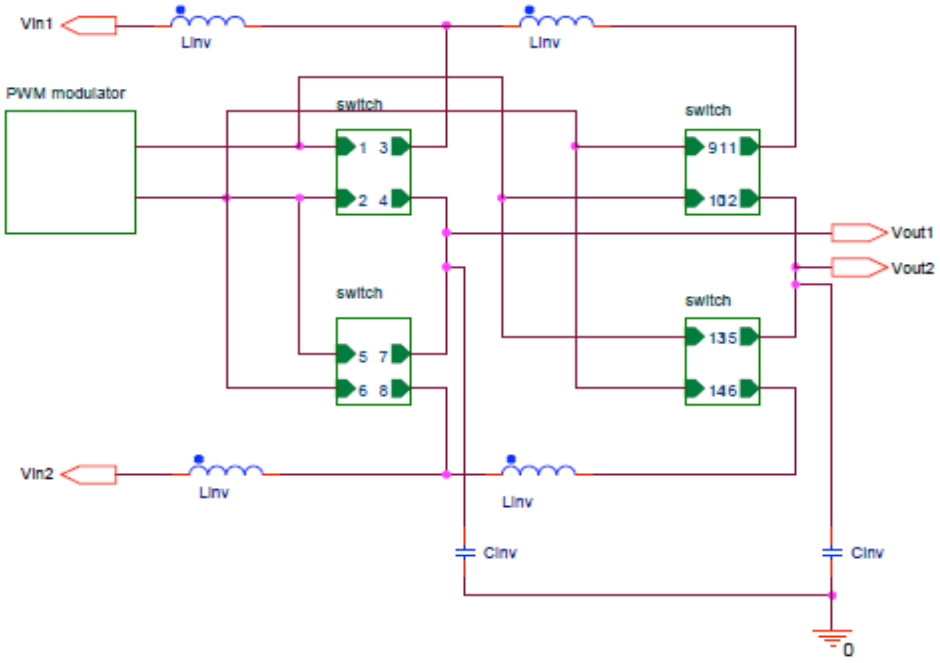

Fig. 6. PSpice model of the inverter.

Table 3. Parasitic parameters of the inverter

Parasitic capacitance to ground [pf]	C_{inv}	150
Parasitic inductance of the connecting wires [nH]	L_{inv}	10

Table 4. Parasitic parameters of the IGBT

Conduction parasitic inductance [nH]	L_{on}	10
Series resistance Rs [mΩ]	R_s	100
Shunt Resistance [Ω]	R	100
Shunt capacitance [nF]	C	1

C. Model of the Power Devices

The IGBT is modelled by an ideal switch in series with an L-R branch formed of a conduction parasitic inductance, Lon, and a resistance Rs to take into consideration the commutation losses. The commutation speed of the power device is reproduced by an R-C branch connected in parallel to the device. The model is given in Fig. 7. The values of the parasitic parameters are given in Table 4.

The PCU is supposed to be in proximity of the PV panel, for this reason the models of cables can be neglected without affecting the validity of the analysis as explained in [15].

5. Results

Based on the modelling defined in the previous sections, a global circuit model, suitable for the forecasting of CM currents, of the PV plant has been designed and implemented in PSpice. One guess is that the PV plant is grid connected through a line inductance L=6mH. The corresponding circuit model is sketched in Fig.8. Power grid connection is simply modeled by a sinusoidal generator Vg, a resistive load Rl and on ohmic-inductive branch Rg-Lg accounting for the connection cables.

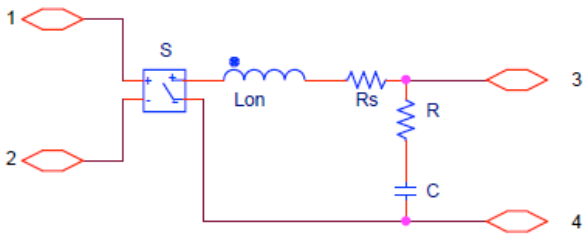

Fig.7. PSpice model of the IGBT.

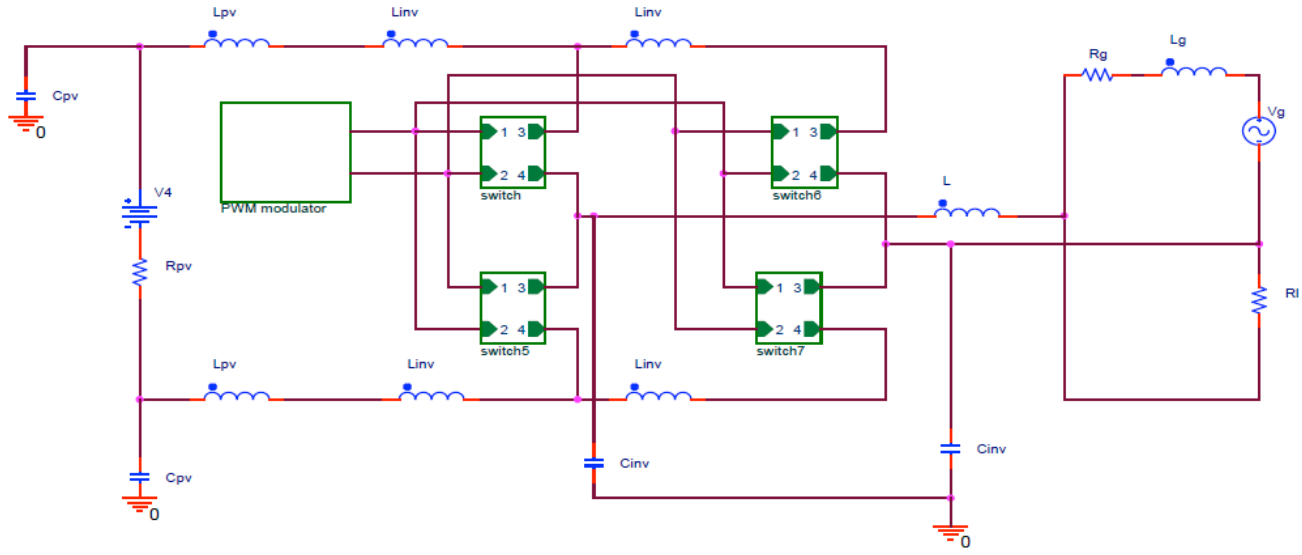

Fig. 8. PSpice global model of the grid-connected PV plant.

Figure 8 shows the PSpice model of the complete grid connected plant. No parasitic couplings through ground are considered on the grid side; this case is very likely when a LF transformer is present in the plant.

The voltage waveforms of the PV plant were simulated by taking into account the PWM logic; Fig. 9 shows the voltage waveform at inverter terminals, and Fig. 10 shows in a zoom the voltage rapid transition due to commutation.

In Fig.11 the current feeding the power grid is reported, the non-null value exhibits that there is a power flow from PV system to grid.

The CM voltage waveform, at the inverter output, in a 20 ms period is shown in Fig.12; a zoom showing the oscillations due to the switching of a component is also represented in Fig. 13.

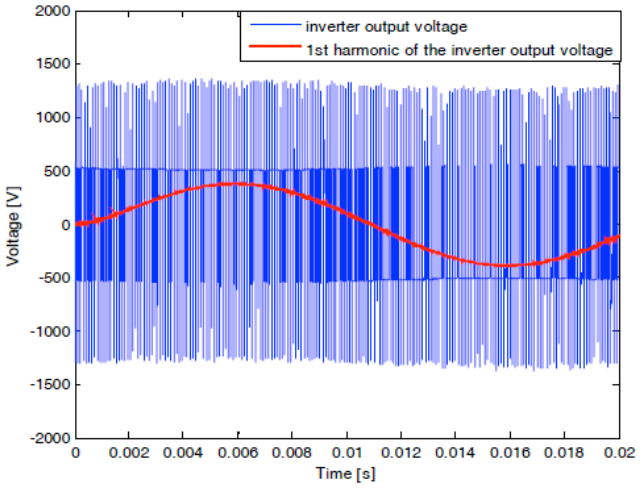

Fig.9. Voltage at the output of the inverter.

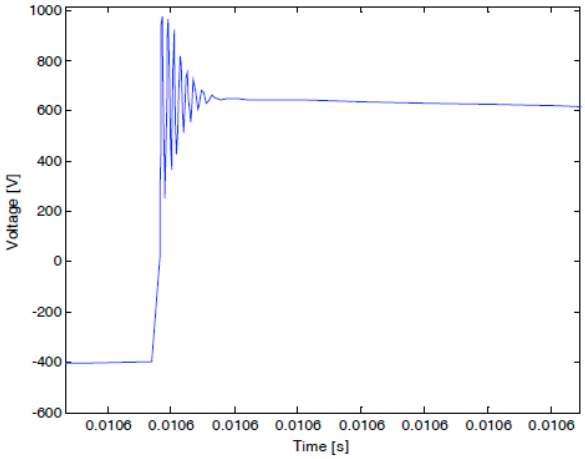

Fig.10. Zoom of the voltage at the inverter output.

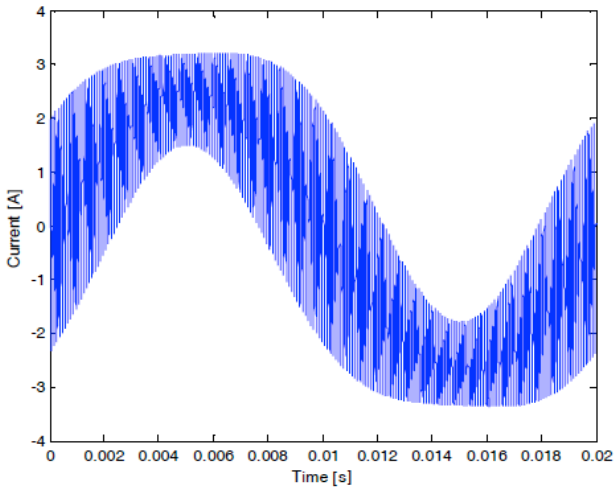

Fig.11. Current on the line inductance.

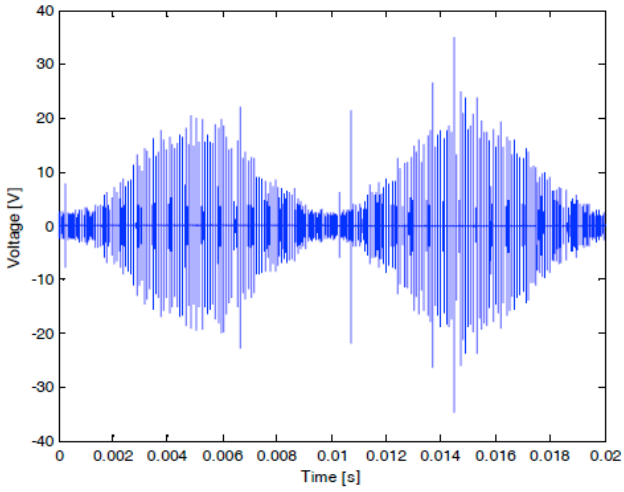

Fig. 12.CM voltage at the inverter output.

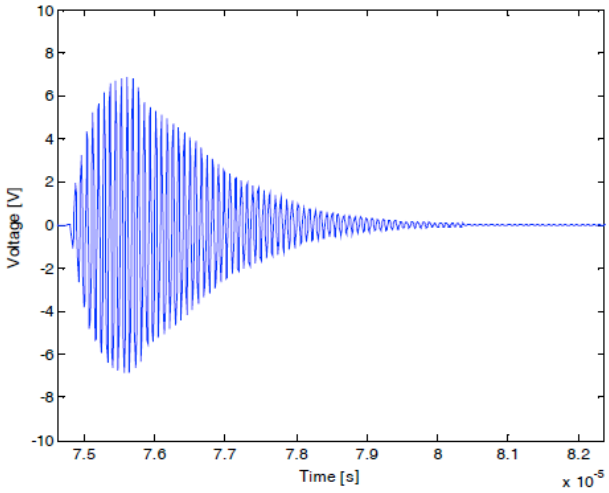

Fig.13. Zoom of a single pulse in the CM voltage.

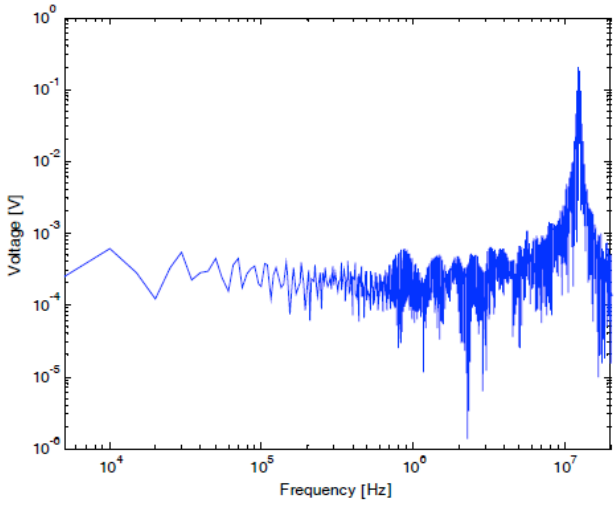

Fig.14. Frequency spectrum of the CM voltage.

As first result of this study, it should be put in evidence that, even in time domain representation, the existence of oscillations due to the fast PWM technique highlights the presence of high frequency voltage harmonics, embracing a path by capacitors and inductors. It has to be noted is that the current, flowing in this loop, does not find voluntary and controllable impedances in its path, and could also reach resonance conditions, potentially dangerous.

The frequency spectrum of the CM voltage is shown in Fig.14. It presents harmonics at frequencies multiple of the switching frequency and a strong resonance at about 12 MHz. The same analysis has been realized also for the current. The representation of CM current in the path between solar panels and inverter for an interval of 20 ms in given in Fig.15; The magnification of a current pulse is given in Fig.16.

Again, it can be stated that there are oscillations for the CM current. These oscillations exhibit a short period corresponding to a high frequency. The waveforms show oscillations with a period about 80 ns corresponding to a frequency of 12.5 MHz. Depending on the length of the path in which the CM current flows a radiated effect can occurs. Considering that the wavelength of the oscillating frequency, equal to 24m, is comparable with the distance between the panel and the inverter, an equivalent radiation antenna can result as a non-intentional noise source.

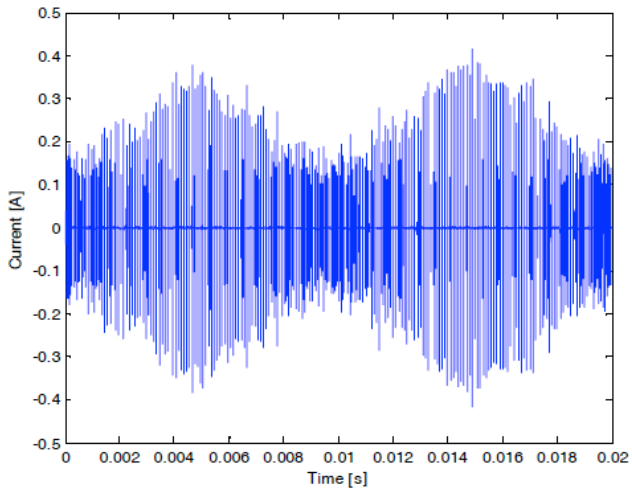

Fig.15. CM current in the loop between the PV array and the inverter.

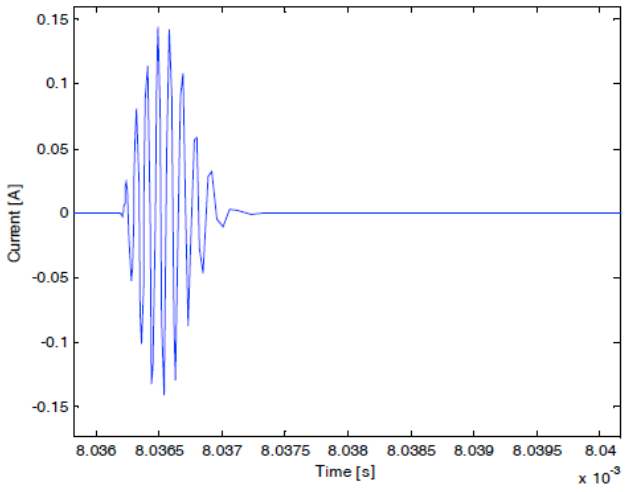

Fig.16. Zoom of a single pulse in the CM current.

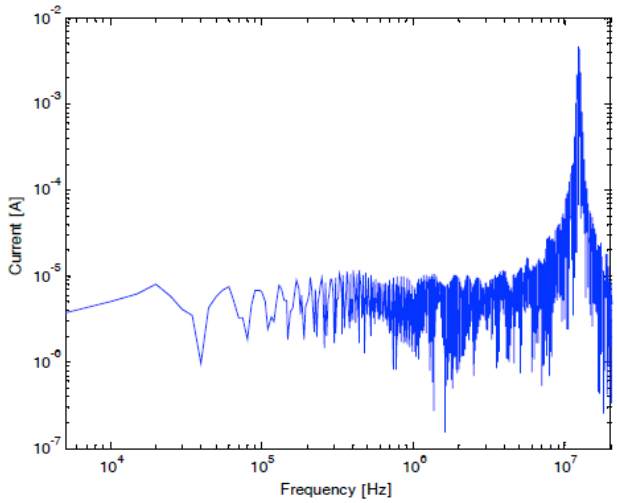

Fig. 17. Frequency spectrum of the CM current.

A similar result can be obtained by considering the resonance period T of a part of the system:

$$T = 2\pi\sqrt{L_{PV}C_{PV}} = 53ns$$

This result allows to support the theory for which the parameters that mainly affect the CM current propagation are due to the parasitic coupling of the solar panel configuration.

Another key point is the absence of DC component as shown in Fig. 16. Such absence of zero frequency is expected, since it is a typical behavior of damped resonant circuits.

Finally, the frequency spectrum of the CM current is shown in Fig.17, where the resonance at 12 MHz is present, as well.

6. Conclusion

This paper traces out the modeling of high frequency behavior of a PV system, useful to evaluate the common mode voltage and current, generated by the employment of a PWM technique in the power conversion unit.

A lumped parameter approach has been followed to describe the principal devices used in the system. Particular attention has been devoted to the modeling of PV array, experimental results measured in a laboratory test bench allowed to define the performance of a single PV panel. The complete PV plant model has been implemented in PSpice environment and the common mode ground currents have been obtained in simulation both in time and frequency domain.

The principal results of this analysis is that a resonance path at about 12.5 MHz is present in the system; it supports the generation of common mode resonance voltages and currents due to fast switching of the inverter; the common mode ground current has a time period that can be identified by the parameters of the photovoltaic array system.

References

[1] T. Esram, P. L. Chapman, “Comparison of Photovoltaic Array Maximum Power Point Tracking Techniques”, IEEE trans on Energy C. , vol. 22, n.. 2, June 2007

[2] M.C. Di Piazza, M. Pucci, G. Vitale, “Intelligent power conversion system management for photovoltaic generation”, Sustainable Energy Technologies and Assessments, (2013), 2, 19-30.

[3] F. Iov, F. Blaabjerg, “Power Electronics for Renewable Energy Systems”, POWERENG 2009 Lisbon, Portugal, March 18-20, 2009

[4] Frede Blaabjerg, Florin Iov, Remus Teodorescu, Zhe Chen, “Power Electronics in Renewable Energy Systems”, EPEPEMC 2006, Portoroz, Slovenia.

[5] S. B. Kjaer, J. K. Pedersen, F. Blaabjerg,“ A Review of Single-Phase Grid-Connected Inverters for Photovoltaic Modules“, IEEE trans on Industry Applications, vol. 41, n. 5,September/October 2005.

[6] J. M. Carrasco, L. Garcia Franquelo, J. T. Bialasiewicz, E.Galván, R. C. Portillo Guisado, M.. Á. Martín Prats, J. I. León, N. Moreno-Alfonso, “Power-Electronic Systems for the Grid Integration of Renewable Energy Sources: A Survey” , IEEE trans. On Industrial Electronics, vol. 53, n. 4, August 2006.

[7] R. Gonzalez, J. Lopez, P. Sanchis, and L. Marroyo, “Transformerless inverter for single-phase photovoltaic systems,” IEEE Trans. Power Electron., vol. 22, no. 2, pp. 693–697, Mar. 2007.

[8] Mohamed Amine Abdourrziq, Mohammed Ouassaid, Mohamed Maaroufi, “Single-Sensor Based MPPT for Photovoltaic Systems”, International Journal of Renewable Energy Research-IJRER, Vol 6, No 2 (2016): Vol6

[9] Wassila Issaadi, "An Improved MPPT Converter Using Current Compensation Method for PV-Applications", International Journal of Renewable Energy Research-IJRER, Vol 6, No 3 (2016): Vol6

[10] S.A. Rizzo, N. Salerno, G. Scelba, A. Sciacca, "Enhanced Hybrid Global MPPT Algorithm for PV Systems Operating under Fast-Changing Partial Shading Conditions",International Journal of Renewable Energy Research-IJRER, Vol.8, No.1, March, 2018

[11] G. Schettino, S. Benanti, C. Buccella, M. Caruso, V. Castiglia, C. Cecati, A.O. Di Tommaso, R. Miceli, P. Romano and F. Viola, "Simulation and Experimental Validation of Multicarrier PWM Techniques for Three-phase Five-Level Cascaded H-bridge with FPGA Controller", International Journal of Renewable Energy Research-IJRER,Vol.7, No.3, 2017

[12] R. Araneo, S. Lammens, M. Grossi, S. Bertone, “EMC Issues in High-Power Grid-Connected Photovoltaic Plants”, IEEE trans on Electromagnetic compatibility, vol. 51, n. 3,August 2009.

[13] H. Xiao, S. Xie, "Leakage Current Analytical Model and Application in Single-Phase Transformerless Photovoltaic Grid-Connected Inverter", IEEE trans on Electromagnetic compatibility, vol. 52, n. 4, Nov. 2010

[14] E. Gubia, P. Sanchis, A. Ursua, J. Lopez, and L. Marroyo, "Ground current in single-phase transformerless photovoltaic systems," in Progress in Photovoltaics: Research and Applications. New York: Wiley, pp. 629–650, 2007.

[15] M. C. Di Piazza, A. Ragusa, G. Vitale, "Design of Grid-Side Electromagnetic Interference Filters in AC Motor Drives with Motor-Side Common Mode Active Compensation", IEEE Transactions on Electromagnetic Compatibility, vol. 51, N. 3 Part 2, August 2009, Page(s):673 – 682.